Since January 2020 Elsevier has created a COVID-19 resource centre with free information in English and Mandarin on the novel coronavirus COVID-19. The COVID-19 resource centre is hosted on Elsevier Connect, the company's public news and information website.

Virology 559 (2021) 1–9

Contents lists available at ScienceDirect

Virology

journal homepage: www.elsevier.com/locate/virology

The development and kinetics of functional antibody-dependent cell-mediated cytotoxicity (ADCC) to SARS-CoV-2 spike protein

Xuemin Chen [a,b], Christina A. Rostad [a,b], Larry J. Anderson [a,b], He-ying Sun [a], Stacey A. Lapp [a,b], Kathy Stephens [a], Laila Hussaini [a], Theda Gibson [a], Nadine Rouphael [c], Evan J. Anderson [a,b,c,*]

[a] Division of Infectious Diseases, Department of Pediatrics, Emory University School of Medicine, Atlanta, GA, United States
[b] Center for Childhood Infections and Vaccines, Children's Healthcare of Atlanta, Atlanta, GA, United States
[c] Division of Infectious Diseases, Department of Medicine, Emory University School of Medicine, Atlanta, GA, United States

ARTICLE INFO

Keywords:
SARS-CoV-2
Antibody-dependent cell-mediated cytotoxicity (ADCC)
COVID-19
Spike (S) protein
NK cells
FcγRIIIa receptor (CD16)

ABSTRACT

Since the COVID-19 pandemic, functional non-neutralizing antibody responses to SARS-CoV-2, including antibody-dependent cell-mediated cytotoxicity (ADCC), are poorly understood. We developed an ADCC assay utilizing a stably transfected, dual-reporter target cell line with inducible expression of a SARS-CoV-2 spike protein on the cell surface. Using this assay, we analyzed 61 convalescent serum samples from adults with PCR-confirmed COVID-19 and 15 samples from healthy uninfected controls. We found that 56 of 61 convalescent serum samples induced ADCC killing of SARS-CoV-2 S target cells, whereas none of the 15 healthy controls had detectable ADCC. We then found a modest decline in ADCC titer over a median 3-month follow-up in 21 patients who had serial samples available for analysis. We confirmed that the antibody-dependent target cell lysis was mediated primarily via the NK FcγRIIIa receptor (CD16). This ADCC assay had high sensitivity and specificity for detecting serologic immune responses to SARS-CoV-2.

1. Introduction

SARS coronavirus-2 (SARS-CoV-2), the *betacoronavirus* that emerged in Wuhan, China in December 2019, has become a global public health concern due to its rapid worldwide spread. The disease caused by SARS-CoV-2, named coronavirus disease 2019 (COVID-19), is characterized by severe pulmonary disease, particularly in older adults and those with pre-existing comorbidities. According the COVID-19 Data Repository by The Center for Systems Science and Engineering (CSSE) at Johns Hopkins University, as of October 15, 2020, over 38 million people had been infected with SARS-CoV-2 globally. Although 26 million people had recovered from the disease, there had been over one million deaths (JKU, 2020). Currently, the primary protective humoral immune response is thought to be neutralizing antibodies and primarily those that prevent infection by blocking viral attachment and cellular entry (Atyeo et al., 2020; Dogan et al., 2020; Gao et al., 2020a; Robbiani et al., 2020). Some studies have suggested that administration of human plasma collected from previously infected individuals with high virus-specific antibody titers could also be used to treat active infection or alter disease progression (Abolghasemi et al., 2020; Atyeo et al., 2020; Bloch, 2020).

Although neutralizing antibodies are accepted as correlates of protective immunity against many viruses, neutralizing antibodies represent only a subset of the antibody repertoire that has anti-viral functions. For example, there are a number of antiviral functions mediated by Fc receptor binding to immune cells, including antibody-dependent cell-mediated cytotoxicity (ADCC), antibody-dependent cellular phagocytosis (ADCP), antibody-dependent complement deposition (ADCD), and antibody-dependent neutrophil phagocytosis (ADNP). In ADCC, antibodies bind to viral antigens on the surface of infected target cells. Effector immune cells, most commonly natural killer (NK) cells, bind to the antibodies via Fc receptors on their surface and then undergo degranulation releasing perforin and granzyme lysing infected cells. ADCC has been observed after infection with a number of viral pathogens (Garcia et al., 2006; He et al., 2016; Singh et al., 2018), and it has been demonstrated to be an important component of protective immunity against HIV-1 (Asokan et al., 2020; Haynes et al., 2012; Su et al., 2019), Influenza (Gao et al., 2020b; Zheng et al., 2020), Ebola (Wagstaffe et al., 2019) and may have a role in other viral infection (Chen, 2020). Since little is known about the role of ADCC in SARS-CoV-2

* Corresponding author. Division of Infectious Diseases, Department of Pediatrics, Emory University School of Medicine, Atlanta, GA, United States.
E-mail address: evanderson@emory.edu (E.J. Anderson).

https://doi.org/10.1016/j.virol.2021.03.009
Received 18 November 2020; Received in revised form 12 February 2021; Accepted 14 March 2021
Available online 19 March 2021

infections, we developed a functional SARS-CoV-2 spike (S) protein-based ADCC assay to assess the development and kinetics of antibodies after SARS-CoV-2 infection.

2. Materials and methods

2.1. Serum samples

Healthy adults or adults with PCR-confirmed SARS-CoV-2 infection were prospectively enrolled for blood sample collection into Emory IRB-approved protocols IRB00045690 or IRB00022397, respectively. The study included 61 serum samples from 40 patients with SARS-CoV-2 infection confirmed by RT-qPCR (50% male, 50% females; the median age is 48, ranging from 21 to 77): 58 samples collected in the convalescent phase (>14 days from onset of symptoms, range 23–132 days) and 3 samples were collected in the acute phase (≤14 days after onset of symptoms). 21 patients provided 2 specimens. In seventeen participants, the first specimen was collected 30–62 days after onset of symptom and second one was collected at 3 months later. For the other four patients, who provided 2 serum samples separated by < 30 days, the first specimen collected between 7 and 23 days and the second collection between 13 to 33 days post symptom onset. We also tested 15 serum samples from healthy adults collected before the COVID-19 pandemic as negative control specimens. All samples underwent virus and complement inactivation by heating at 56 °C for 60 min prior to analysis.

2.2. SARS-CoV-2 S protein and reporter gene constructs

An enhanced green fluorescent protein (EGFP)-ires-Luciferase reporter gene derived from plasmid pHAGE PGK-GFP-Luciferase-w (addgene Plasmid #46793) was cut with NotI and ClaI and then blunted by Klenow Fragment. The blunt fragment was introduced into the EcoRV site of plasmid pcDNA4/TO (Invitrogen, Carlsbad CA) to generate plasmid pcDNA4/TO GFP-ires-Luc. The codon-optimized SARS-CoV-2 spike gene (NC_045512.2) (Genscript) was then cloned into the pCDNA5/TO (puro) plasmid at the *Bam*HI and XhoI sites and was named "pcDNA5/TO (p) CoV2_S."

2.3. Target cells

The procedure for making a reporter-only cell line with dual EGFP and luciferase expression was published previously (Chen, 2020). The reporter-only cells were then transfected with pcDNA5/TO (p) CoV2_S. Following puromycin selection single clones were expanded and characterized by flow cytometry using convalescent serum from patients with COVID-19. After characterization, the individual clone with the highest surface expression of spike protein was amplified and named the "SARS CoV-2 S target cell line." The SARS CoV-2 S target cell line was subsequently characterized by flow cytometry. First, the cells were induced with doxycycline for 20 h, then incubated with serum specimens for 1 h at 4 °C, and subsequently stained with Allophycocyanin (APC)-conjugated goat anti-human IgG (H + L) antibody (Jackson ImmunoResearch Laboratory: #109-136-098) for 30 min. Flow cytometry was performed to confirm the cellular expression of Spike proteins and EGFP. Images were acquired on an LSR II flow cytometer (BD Biosciences) and analyzed with FlowJo software (Tree Star). These cell lines were used for subsequent experiments.

Western blotting was performed on induced target cells using polyclonal mouse antisera to the spike protein receptor binding domain (RBD) followed by IRDye 800CW Donkey anti-mouse IgG secondary antibodies (LI-COR #926–32212). To generate the antisera, five BALB/c mice were inoculated intramuscularly with 10 μg each of alum-adjuvanted (Alhydrogel adjuvant 2%, Invitrogen) purified SARS-CoV-2 RBD. The RBD was produced as previously described (Suthar et al., 2020) and was kindly given by Jens Wrammert. The mice were boosted at 3 weeks following initial inoculation with 10 μg RBD protein. Serum was collected from submandibular bleeding on day 21 following the boost. All animal experiments were conducted according to approved IACUC protocols at Emory University (PROTO202000026).

2.4. Effector cells

The effector cells utilized for the assay were from the CD16-176 V-NK-92 cell line (ATCC: PTA-6967) which have high expression of CD16 on the cell surface. The NK-92 cell line (ATCC CRL-2407) that lacks CD16 was used as an effector control cell line. The effector cells were maintained in NK complete medium (Alpha MEM without ribonucleotides and deoxyribonucleosides media containing 0.2 mM of Myo-inositol, 0.1 mM of 2-Mercaptoethanol, 0.02 mM of folic acid, and 12.5% each of heat-inactivated horse and fetal bovine serum) supplemented with 200 IU/ml of human recombinant IL-2 (R&D system: #202-IL-050).

2.5. ADCC assay

ADCC assay was conducted as described previously (Chen, 2020). The serum samples were serially diluted in duplicate in 96-well V-bottom plates with AIM V™ (Gibco 12055091) medium starting at 1:30 with 3-fold dilutions. The effector: target (E: T) cell ratio of 2:1 and 4 h incubation time were the optimal experimental condition. After addition of Britelite Plus luciferase reporter reagent (PerkinElmer) the plate was incubated for 5 min and Relative Luminescence Units (RLU) was read on a luminometer (TopCount NXT Luminescence Counter).

2.6. ADCC calculation

The percent lysis of target cells was calculated for each well using the following formula:

ADCC (%) = [RLU* (no antibody) - RLU (with antibody)]/RLU (no antibody)] × 100.

2.7. Statistical analysis

The specificity and sensitivity of ADCC assay was analyzed by receiver operating characteristic (ROC) curve. The assay performance using sera from adults with PCR-confirmed SARS-CoV-2 and healthy control adults at different serum dilutions was analyzed. We chose to use the cutoff value as the percentage of target cell lysis that gave 100% specificity at all dilutions in the ROC analysis. All the statistics were performed with GraphPad Prism (version 7.0). The correlation was calculated using a nonparametric Spearman correlation test. Statistical comparisons were made using Student's t-tests. P-values ≤0.05 were considered statistically significant.

3. Results

3.1. Development of a SARS-CoV-2 ADCC target cell line

We generated a stably transfected dual-reporter SARS-CoV-2 S target cell line with inducible protein expression regulated by tetR. To accomplish this, we sequentially transfected T-Rex-293 cells with plasmids encoding EGFP and luciferase, followed by codon-optimized SARS-CoV-2 S and selected for high-expressing clones. We found that S protein and reporter protein expression were tightly regulated by tetR. Upon induction with doxycycline, EGFP could be visualized in real time via fluorescence microscopy (Fig. 1A). The inducible expression of luciferase could also be measured using a luminometer, and expressed as Relative Luminescence Units (RLUs). Without doxycycline induction, no luciferase activity was detected (Fig. 1B). The expression of spike protein in SARS-CoV-2 S ADCC target cells was characterized by Western blot using polyclonal anti RBD antibody (Fig. 1C). Full length S protein was clearly visible in cell lysate of S target cell with doxycycline

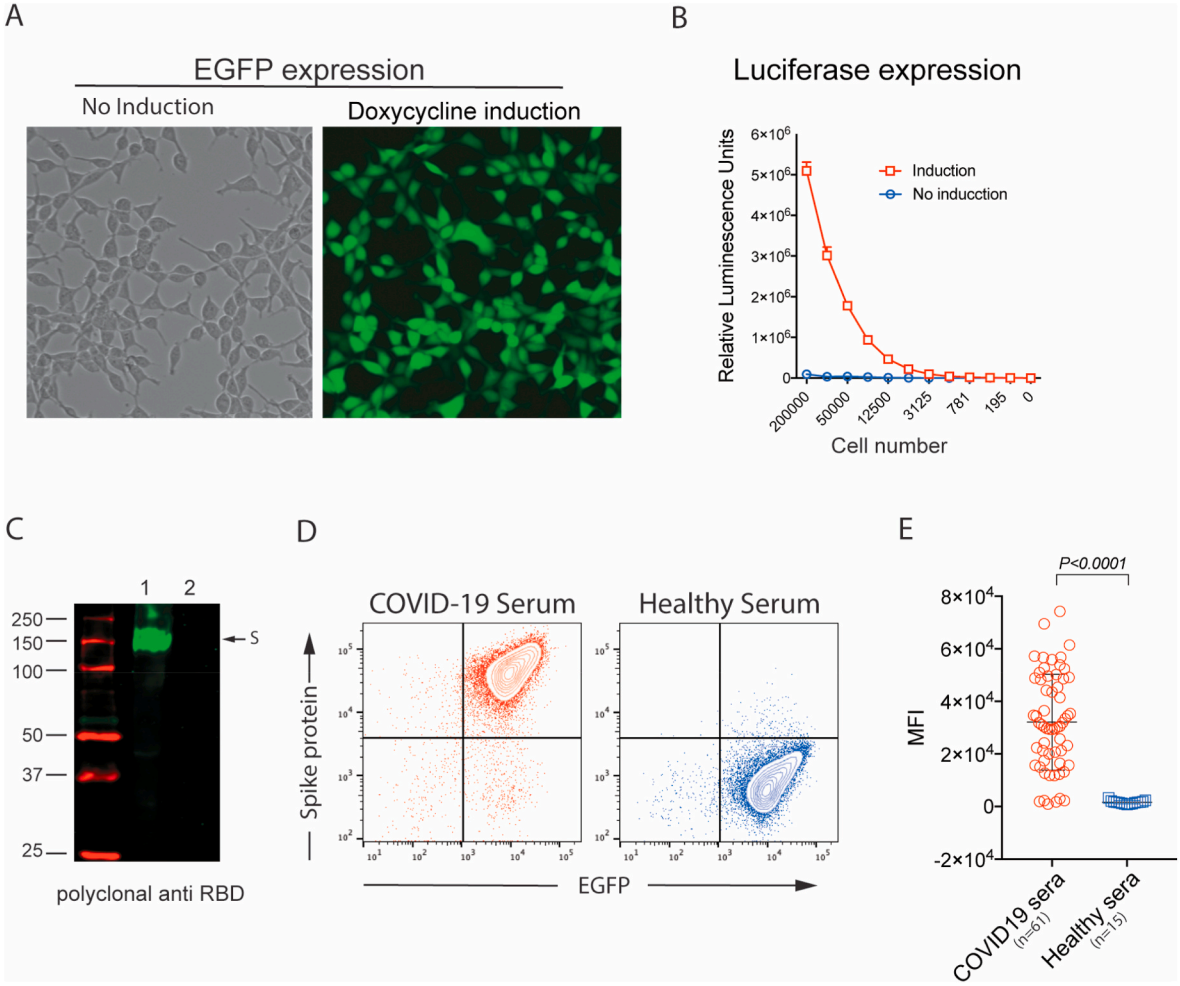

Fig. 1. Expression of SARS-CoV-2 spike (S) protein and reporter proteins (enhanced green fluorescent protein [EGFP] and luciferase) from SARS-CoV-2 ADCC target cell line. The inducible SARS-CoV-2 S protein dual-reporter target cell line was analyzed for protein expression before and after induction with doxycycline. EGFP protein expression was visualized via fluorescence microscopy (A). Luciferase expression was measured in relative luminescence units (RLUs) using a TopCount Luminescence Counter (B). Spike protein expression was analyzed by Western blot using polyclonal anti-RBD antibody (C). Lane 1 is the cell lysates from SARS-CoV-2 ADCC spike target cell with doxycycline inducted and lane 2 is from the SARS-CoV-2 Spike ADCC target cell without doxycycline induction. Spike protein and EGFP expression were analyzed by flow cytometry using a COVID-19 convalescent serum and a healthy control serum (D). Antibody reactivity against spike protein on the target cell surface was measured as mean fluorescence intensity (MFI) using sera from adults with PCR-confirmed COVID-19 (circle red; n = 61) and sera from healthy adult controls (square blue; n = 15) (E). Line shows mean ± standard deviation. Statistical comparisons were made using Student's t-test. $P < 0.05$ was considered statistically significant.

induction. In contrast S protein was not detected in the cell lysate without induction. We then confirmed that the S protein expression was on the target cell surface by flow cytometry using a serum sample from patient with PCR-confirmed COVID-19. One healthy serum was used as isotype control (Fig. 1D). To further assess antibody binding to S protein on target cells we tested our cohort of 61 COVID-19 specimens by flow cytometry and used MFI to quantify binding activity (Fig. 1E). The MFI determined from 15 healthy adult control was used to compare with that from COVID-19 patients. The difference of binding ability between the patient's group and healthy group is significant at $p < 0.0001$. Note that 5 specimens from COVID-19 patients had MFI values similar to the control specimens.

3.2. Development of a SARS-CoV-2 ADCC assay

We then developed our ADCC assay using a subset of serum samples from our cohort, which included 5 adults with PCR-confirmed COVID-19 and 5 healthy adult controls. The 5 sera from adults with PCR-confirmed COVID-19 were chosen based on their different levels of antibody binding to SARS-CoV-2 S target cells, as measured by flow cytometry. The sera were tested at serial 3-fold dilutions beginning with a 1:30 dilution in a 96-well plate format. We measured ADCC activity of these sera using target cells with and without S protein expression and using effector cells with (NK CD16$^{(+)}$) and without (NK-92) CD16 (FcγRIIIa receptor) expression on the surface. All 5 sera from adults with PCR-confirmed COVID-19 elicited lysis of S protein-expressing target cells by NK CD16$^{(+)}$ effector cells (Fig. 2A–E). The amount of target cell lysis varied among the specimens with a maximum lysis of 83% (Fig. 2B). All sera elicited lower ADCC at the 1:30 dilution than at the 1:90 and 1:270 dilutions, which we attributed to prozone effect. As expected, replacing NK CD16$^{(+)}$ effector cells with the NK-92 CD16-negative cells dramatically reduced target cell lysis. Reporter-only target cells lacking S surface expression also did not undergo appreciable cell lysis in the presence of SARS-CoV-2 sera and NK CD16$^{(+)}$ effector cells. (Fig. 2A–E). Similarly, the 5 healthy control serum samples did not elicit target cell lysis, either in the presence of NK CD16$^{(+)}$ effector or NK-92 control cells (Fig. 2F–J). Altogether, these data demonstrate that anti-Spike protein antibodies in sera from adults with PCR-confirmed SARS-CoV-2 elicit ADCC of target cells via FcR binding to NK effector cells. To assess repeatability of results, we tested two different human antibodies anti-

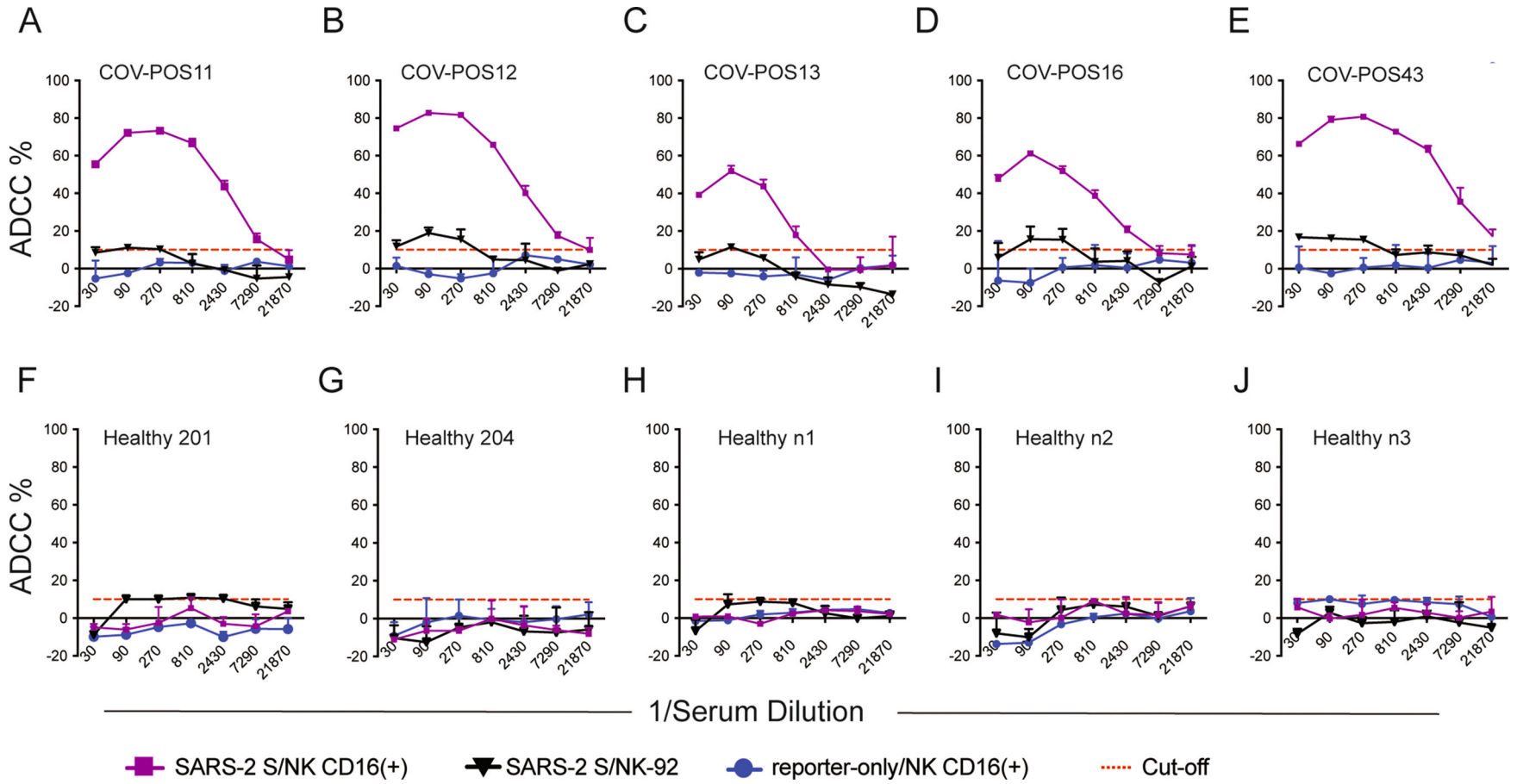

Fig. 2. ADCC of SARS-CoV-2 S target cells is mediated by COVID-19 serum via F_c receptor binding, and ADCC was not observed in the reporter-only control cell line. SARS-CoV-2 S target cells and Reporter-only cells were incubated with individual COVID-19 sera and NK $CD16^{(+)}$ effector cells or NK-92 cells lacking CD16 on the surface. Fig. 2A to 2.E shows the percentage of cell lysis elicited by 5 unique COVID-19 serum samples. Fig. 2F to 2.J shows ADCC from 5 healthy control sera. The serum dilution is indicated on the x-axis. Dotted red lines indicate the 10% cutoff for calculating endpoint titers. All samples were run in duplicate, and data represent the mean ± standard deviation of %ADCC cell lysis.

SARS-CoV-2 spike RBD monoclonal antibodies (M180 and S35) and one human anti-Ebola glycoprotein monoclonal antibody (kz52, active in Ebola ADCC) (Figure S1) on two different days. The killing activity at each dilution for both monoclonal antibodies was very similar for both days indicating good assay repeatability.

We next examined ADCC using all 61 serum samples from our cohort of adults with PCR-confirmed SARS-CoV-2 and 15 healthy adult controls. Serial serum dilutions were made from 1:30 to 1:21,870. ADCC activity was observed in 56 of 61 SARS-CoV-2 serum samples, with cell lysis peaking at the 1:90 or 1:270 dilution. Some degree of a prozone effect was observed with most of the 56 ADCC positive sera. We did not detect ADCC activity in the 5 COVID-19 sera which lacked S-protein binding by flow cytometry as demonstrated in Fig. 1E. The 15 healthy control sera had maximum cell lysis <10%. We compared the ADCC activity of COVID-19 and healthy control sera at each serum dilution using Welch's unpaired t-tests. We found significant differences between the two groups at each serum dilution even reaching the serum dilution of 1:7290 (Fig. 3A).

To examine the performance of the assay, receiver operating characteristic (ROC) curves were built separately for each serum dilution with the ADCC data obtained from all serum samples (Fig. 3B). The area under the corresponding experimental ROC (AUC) for each serum dilution was calculated with its 95% confidence interval (95%CI). The best AUC value (0.97) was seen at the 1:90 serum dilution. In comparison, the AUC value was slightly lower (0.96) at the 1:30 dilution, which we attributed to the prozone effect. Even at a serum dilution of 1:270, the AUC was >0.91, indicating the assay highly discriminated patients with prior SARS-CoV-2 infection vs. healthy controls.

The cutoff values for endpoint titers at each dilution were calculated and are shown in Table 1. At a specificity of 100%, the sensitivity was 84% at 1:30, 85% at 1:90 and 72% at 1:270 serum dilution. As expected, the assay sensitivity decreased as the serum dilution further increased. Based on the ROC analysis and the fact of that the 15 healthy control sera had maximum cell lysis <10% at each dilution, we chose 10% (see Table 1) as the cutoff value for ADCC activity. The highest dilution that had ADCC activity >10% was considered the endpoint titer for that specimen.

3.3. Measurement of SARS-CoV-2 ADCC antibody titers following infection

Using the optimized cutoff value, the ADCC endpoint titers specific to SARS CoV-2 S protein in sera from adults with PCR-confirmed SARS-CoV-2 vs. healthy controls were determined. Fifty-six of 61 patient sera had detectable ADCC antibodies, with endpoint titers ranging from 74 to 27,201. As described above that there were 5 specimens without detectable ADCC antibody response and the titers for these specimens were under 30. Among these, 4 specimens were collected from 4 PCR confirmed patient between 30 to 69 days post symptom onset. One specimen collected at 112 days post symptom onset from a patient who had an ADCC titer of 1529 with the specimen collected at 34 days post symptom onset. ADCC endpoint titers were significantly higher in sera from adults with PCR-confirmed SARS-CoV-2 than healthy controls ($P < 0.0001$) (Fig. 4A). Based on the specimen collected days post symptom onset, we divided the specimens into 3 groups to analyze the kinetics of ADCC antibody response. Of the 61 specimens tested, 3 were collected in less than or equal to 14 days post symptom onset (acute phase), 38 specimens were collected between 15 and 90 days (early convalescent phase) and 20 specimens were collected between 91 and 132 days (later convalescent phase) post symptom onset. The total number of detected ADCC antibody response was 3/3 (100%) in acute phase, 34/38 (89%) in early convalescent phase and 19/20 (95%) in later convalescent phase. The highest average titer was seen in acute-phase specimens (<14 days), with a mean of 14,538 ± 7316 compared with 3148 ± 734 for early convalescent phase and 1176 ± 203 for later convalescent phase ($p = 0.009$ and $p < 0.0001$ respectively). Although there were 4 ADCC negative specimens in early convalescent phase group, the mean ADCC titer in this group is still significantly higher than that of later convalescent phase group ($p < 0.05$) (Fig. 4B).

Additionally, to assess the kinetics of ADCC antibody responses following COVID-19, the ADCC endpoint titers from patients with sequential serum samples collections were plotted vs. days post-symptom onset (Fig. 4C). Twenty-one patients had paired serial samples available for analysis (n = 42). For serum pairs separated by > 30 days the ADCC antibody titers decreased in most (13/17). One patient among these had ADCC antibody titer of 1529 on day 34 after symptom onset which became undetectable on day 112 after symptom onset. The ADCC titer had slightly increased in other 4 of the seventeen. From 4 pairs sera separated by < 30 days, 3 of 4 were collected from acute phase. These specimens demonstrated relatively high levels of early ADCC antibody responses (endpoint titer range from 2172 to 14,553) and ADCC level dramatically increased after 3–10 days (endpoint titer range from 4904 to 27,201). One of 4 patients the ADCC response remained stable over 26 days (endpoint titer from 1859 on 7 days PSO to 1651 on 33 days PSO). Although the numbers of patients and samples available for analysis in the acute-phase were limited, their data demonstrated ADCC antibody response may occur early post-infection and may increase out to about 4 weeks after onset of symptoms.

3.4. Correlation of ADCC activity with pseudoneutralization

To compare the ADCC response with the pseudoneutralizing activity of the patient sera, we used a pseudotyped virus neutralization assay. For this assay, we developed lentiviral particle pseudotyped with the SARS-CoV-2 spike protein and examined the pseudoneutralizing antibody (ID50) titer in 52 COVID-19 patients from the study cohort. We found that the pseudoneutralizing antibody titer strongly correlates with ADCC activity in most specimens (Fig. 5). The correlation with most specimens suggests that the human pseudoneutralizing, binding, and ADCC antibodies are induced to similar levels. The differences suggest not all binding or neutralizing antibodies have ADCC activity and/or some inhibit ADCC. We hypothesize that these differences may help understand COVID-19 immunity.

4. Discussion

We developed a rapid functional SARS-CoV-2 ADCC assay using NK $CD16^+$ effector cells and an inducible dual-reporter target cell line expressing the SARS-CoV-2 spike protein. Since the discovery of ADCC in 1965 (Moeller, 1965), various assays have been developed to measure ADCC activity. These have included ^{51}Cr release assays (Brunner et al., 1968), NK cell activation assays, and ADCC reporter bioassays (Hsieh et al., 2017; Parekh et al., 2012), each of which has limitations. For example, ^{51}Cr release assays require pre-labeling/virus infection of target cells and are subject to high variability. Additionally, ADCC reporter bioassays measure effector cell activation upon FcR binding, but do not measure actual target cell lysis and cytotoxicity. We chose to develop a functional ADCC antibody assay that directly measures target cell lysis and cytotoxicity, modeled after a Zika virus ADCC assay we recently described (Chen, 2020).

We therefore generated a SARS-CoV-2 ADCC dual-reporter target cell line with inducible high expression levels of the Spike protein. To accomplish this, we first transfected the reporter genes of EGFP and luciferase into T-Rex 293 cells. The reporter genes are under the control of the human CMV promoter and two tetracycline operators 2 (TetO2). Their expression is therefore inhibited until induction by tetracycline or doxycycline (Chen, 2020). The inducible line may prevent the potential toxic effects of S protein expression on cells. An advantage of utilizing dual reporters is that EGFP allows real-time visualization of gene expression in living cells via microscopy, whereas luciferase enables rapid, high-throughput quantification of ADCC in 96-well plates. Luciferase expression also enables direct measurement of ADCC, as cell

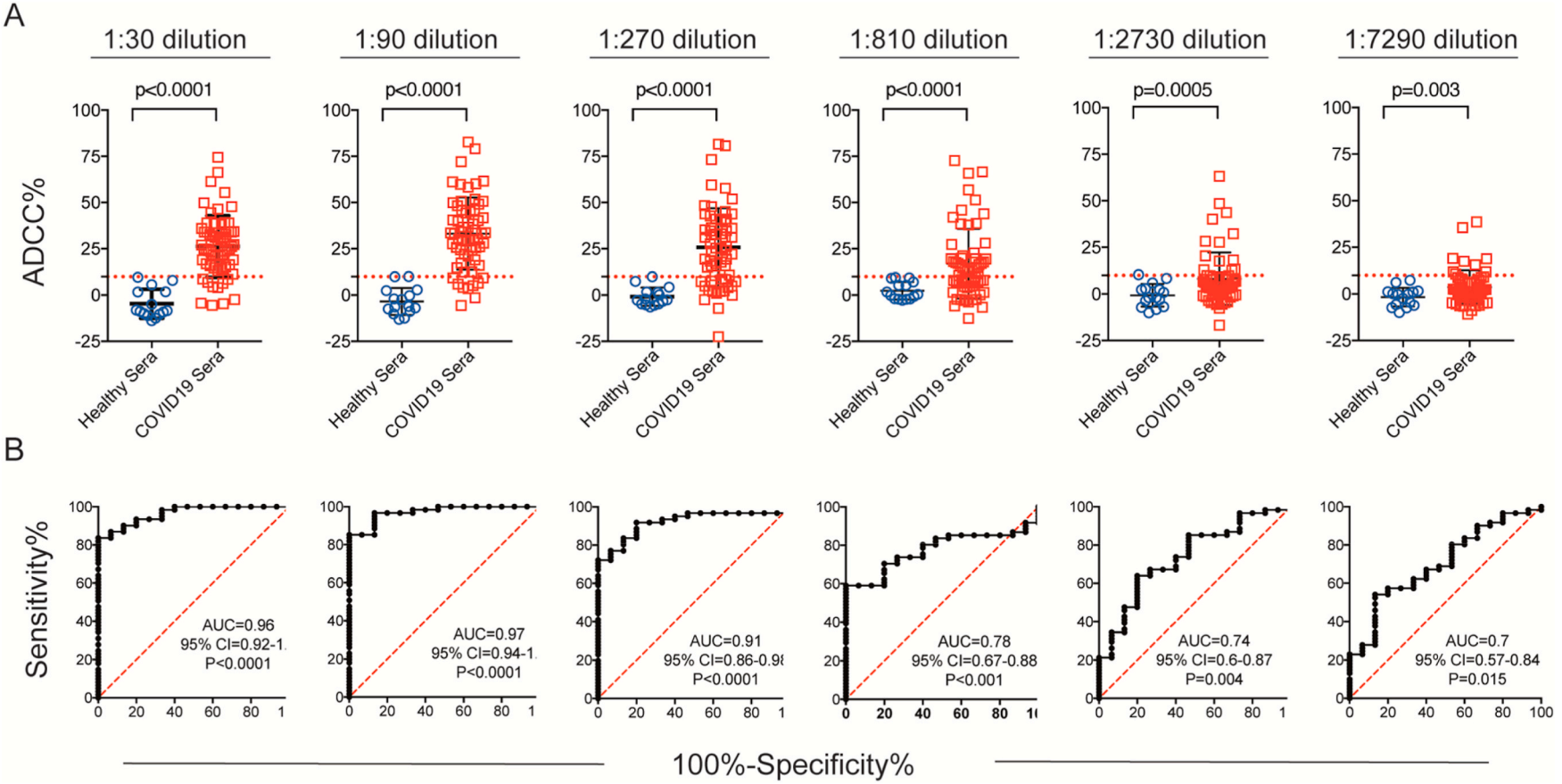

Fig. 3. The sensitivity versus specificity for discrimination of positive and negative sera was analyzed by Receiver operating characteristic (ROC) and area under the ROC curve (AUC) for serial serum dilutions. ADCC activity of 61 serum samples from adults with PCR-confirmed COVID-19 and 15 samples from healthy adult controls were analyzed at serial serum dilutions from 1:30 to 1:7290 (A). Data represent means ± standard deviations. Statistical comparisons were made using Welch's unpaired t-tests, and P-values are shown. Corresponding ROC curves and AUC of percentage of cell lysis are shown in (B). 95% confidence intervals (95%CI) and P-values are indicated.

Table 1
Determination of optimum cutoff values based on ROC curve analysis.

Dilution	Cutoff value	Specificity %	95% CI	Sensitivity %	95% CI
1:30	10.13%	100	78.2%–100%	83.61	71.91%–91.85%
1:90	10.22%	100	78.2%–100%	85.25	73.83%–93.02%
1:270	10.17%	100	78.2%–100%	72.13	59.17%–82.85%
1:810	9.83%	100	78.2%–100%	59.02	45.68%–71.45%
1:2430	11.47%	100	78.2%–100%	21.31	11.86%–33.68%
1:7290	7.485%	100	78.2%–100%	22.95	13.15%–35.5%

lysis is proportional to the decrease in luminescence (RLUs) in each well because luciferase is rapidly degraded in the extracellular fluid (Feeney et al., 2016) and its expression is specific for viable cells.

We chose the S protein because it reliably induces antibodies, including neutralizing antibodies with SARS-CoV-2, is a common component of vaccines (Anderson et al., 2020; Jackson et al., 2020), and is expressed on the surface of infected cells making it a potential target for ADCC antibodies (Barnes et al., 2020; Huo et al., 2020; Walls et al., 2020; Wrapp et al., 2020). Our stable transfected cell line expressed S protein on its surface with good consistency that decreases assay variability. Some studies show a strong association between the ADCC response and antibody binding to the target antigen on the surface of infected cells (Karlsson et al., 2018; Mielke et al., 2019; Smalls-Mantey et al., 2012). In order to explore that antibody binding to the S target cells was proportional to the amount of cell lysis, we compared the correlation of antibody binding MFI with target cell killing in the study sera of the patient cohort with the target cell killing. The result shows positive correlation that indicates the binding was highly predictive of ADCC response ($r = 0.712$; $p < 0.0001$) (Supplemental Figure S2). This suggests some but not all antibody/epitope binding supports ADCC. We do not know the reason for these differences, but they could be due to Fc differences, geometry of the antibody-epitope binding, or other reasons. Understanding the reason for these differences will require further study.

Use of the immortalized NK cell line that stably expresses high-affinity CD16 on its surface (176 V) has been previously used by others and adds to assay reproducibility. This cell line has been shown to be suitable for ADCC assays (Chen, 2020; de Vries et al., 2017; Hassenruck et al., 2018; Mentlik James et al., 2013; Wang et al., 2008). The result was a functional ADCC assay that rapidly assessed cytotoxicity with high sensitivity and specificity. This model of ADCC assay development has now been applied to understanding functional antibody responses to Ebola virus (Singh et al., 2020) Zika virus (Chen, 2020) and now SARS-CoV-2; thus, we hypothesize that this type of functional assay could be similarly applied to understand ADCC responses to a variety of pathogens.

To compare specificity and sensitivity of the assay with a Fc-receptor binding assay, we developed an inducible spike expression cell line using the same parental cells. This cell line was inserted spike gene without GFP and Luciferase dual reporter genes. The cells can express spike protein on the cell surface upon doxycycline induction. We used this cell line as target cells and Jurkat-CD16-NFAT-rLuc reporter cells (Promega) as an effector cells to evaluate ADCC in the present of sera from the same cohort of COVID19 patient or pre-pandemic healthy sera. This assay measures the capacity of a serum to activate NFAT through CD16 in the presence of antigen-expressing target cells. The extent of CD16 activation correlated with our ADCC killing of target cell assay. As with neutralization and binding antibodies, the results are similar for most sera specimens (see Supplementary Figure S3). With the strong correlation of ADCC response from the patient's cohort between the two assays, our assay performed with better specificity and sensitivity.

Previous studies have shown that SARS-CoV-2 specific IgG response increase during the first 3 weeks after symptom onset (Atyeo et al., 2020) and decrease within the subsequent 2–3 months (Shaw et al., 2020). Our kinetics analysis demonstrated that ADCC antibody response can occur by 7 days after symptom onset and continues to increase until early convalescent phase. The high proportion of patients with positive ADCC antibody titer in our cohort had relative higher titer during early convalescent phase (30–90 days after symptom onset) and the titer decreased within 3–4 months after infection. Due to the sample size and the limited time points available for analysis, it is difficulty to establish fully the kinetic pattern of ADCC antibody response after COVID-19

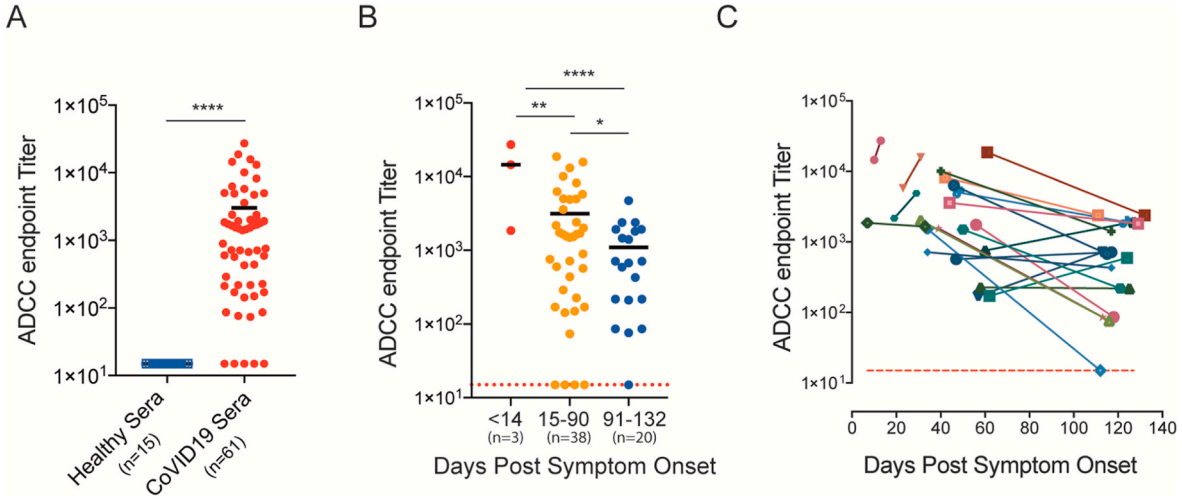

Fig. 4. ADCC antibody endpoint titers and kinetics in adults with PCR-confirmed COVID-19. (A) The ADCC antibody endpoint titers specific to SARS-CoV-2 S protein in sera from adults with PCR-confirmed COVID-19 ($n = 61$) vs. healthy controls ($n = 15$) were determined using a cutoff of 10%. Lines represent the mean of the endpoint titers. Statistical comparisons were made using Welch's unpaired t-test. (B) Specimens were divided into 3 groups based on days post symptom onset. ADCC endpoint titer from each group was determined and compared between the groups. * means $p < 0.05$; ** means $p < 0.01$; *** means $p < 0.001$; **** means $p < 0.0001$. (C) ADCC endpoint titers from all 21 unique patients with PCR-confirmed COVID-19 patients who provided two specimens sequentially were plotted vs. days post-symptom onset. Because the starting dilution of serum was 1:30, this represented the limit of detection (LOD). Samples that did not lyse the cells at the 10% level were plotted at half the LOD, i.e., 15 (red horizontal dashed line). Each line represents an individual patient.

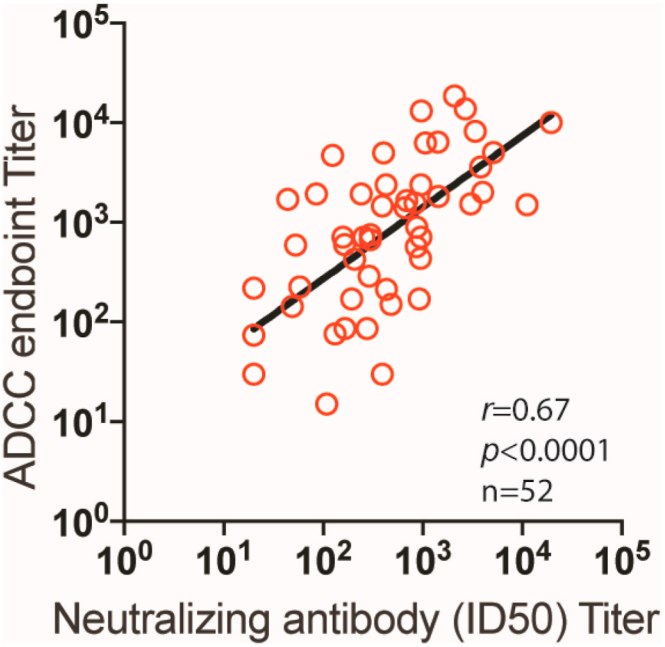

Fig. 5. Correlation between the ADCC response with the pseudoneutralizing activity of the patient sera against SARS-CoV-2 spike protein. The pseudoneutralizing antibody response of 52 COVID-19 patient sera from the cohort were examined using lentiviral particle pseudotyped with spike protein. ADCC and neutralizing activities expressed as the endpoint titers in each individual specimen. A strong correlation was observed between the ADCC antibody endpoint titer to pseudoneutralizing antibody ID50 titer. The correlation was calculated using a nonparametric Spearman correlation test.

infection. However, our finding is consistent with IgG responses observed by prior studies of binding and neutralizing antibody responses to natural infection. The patients in our cohort had mostly mild/moderate COVID-19 disease manifestations, so we were unable to correlate ADCC antibody titers with various clinical outcomes. Additionally, the activity in this assay measures SARS-CoV-2 ADCC against cells transfected with S-protein instead of ADCC activity for SARS-CoV-2 infected cells. It is possible that ADCC activity could differ for SARS-CoV-2 infected cells for a number of reasons, including due to non-S protein based ADCC.

In summary, we developed a rapid, high-throughput SARS-CoV-2 ADCC assay using an inducible dual-reporter target cell line expressing the spike protein and NK CD16$^+$ effector cells, which had high sensitivity and specificity. The assay can be utilized to evaluate functional humoral immune responses to SARS-CoV-2 to better understand the mechanisms of antibody-mediated viral cellular cytotoxicity, immunity, and protection. Understanding serologic correlates of protection against SARS-CoV-2 and the role of ADCC antibodies is critical for the development and evaluation of effective SARS-CoV-2 therapeutics and vaccines.

Author contributions statement

X.C., C.A.R., L.J.A. and E.J.A. proposed and designed the experiments. X.C. performed ADCC experiments. S.A.L. performed mouse experiments and generated polyclonal Spike RBD antiserum. K.S., and L.H. enrolled research subjects and collected clinical specimens. T.G. managed clinical specimen processing and storage. X.C., L.J.A., C.A.R. and E.J.A analyzed the data and discussed the interpretation of results. All authors contributed to review and revisions of the manuscripts.

CRediT authorship contribution statement

Xuemin Chen: Conceptualization, Validation, Formal analysis, Investigation, Data curation, Writing – original draft, Visualization. **Christina A. Rostad:** Conceptualization, Formal analysis, Data curation, Writing – review & editing, Visualization, Supervision. **Larry J. Anderson:** Conceptualization, Formal analysis, Data curation, Writing – review & editing, Visualization, Supervision. **He-ying Sun:** Validation, Data curation, Writing – review & editing. **Stacey A. Lapp:** Validation, Data curation, Writing – review & editing. **Kathy Stephens:** Resources, Data curation, Writing – review & editing. **Laila Hussaini:** Resources, Data curation, Writing – review & editing. **Theda Gibson:** Validation, Data curation, Writing – review & editing. **Nadine Rouphael:** Writing – review & editing, Resources, Visualization, Supervision, Funding acquisition. **Evan J. Anderson:** Conceptualization, Formal analysis, Data curation, Writing – review & editing, Resources, Visualization, Supervision, Funding acquisition.

Declaration of competing interest

E.J.A has received personal fees from AbbVie, Pfizer, and Sanofi-Pasteur for consulting, and his institution receives funds to conduct clinical research unrelated to this manuscript from MedImmune, Regeneron, PaxVax, Pfizer, GSK, Merck, Novavax, Sanofi-Pasteur, Janssen, and Micron. He also serves on a safety monitoring board for Kentucky BioProcessing, Inc and Sanofi-Pasteur.

C.A.R.'s institution has received funds to conduct clinical research unrelated to this manuscript from BioFire Inc, MedImmune, Regeneron, PaxVax, Pfizer, GSK, Merck, Novavax, Sanofi-Pasteur, Janssen, and Micron. She is also co-inventor on patented RSV vaccine technology unrelated to this manuscript, which has been licensed to Meissa Vaccines, Inc.

All other authors, no conflicts.

Acknowledgements

This study was partly funded by the National Institute of Allergy and Infectious Diseases at the National Institutes of Health to the Emory Vaccine and Treatment Evaluation Units [VTEU] HHSN272201300018I and 1 UM1 AI148576-01. Additional support was provided by the Center for Childhood Infections and Vaccines at Emory University and Children's Healthcare of Atlanta, and the Georgia Research Alliance. We would like to thank Hui-Mien Hsiao and Wensheng Li at the Emory Children's Center-Vaccine Research Clinic (ECC-VRC) and Andrew Cheng and Christopher Huerta at the Hope Clinic of the Emory Vaccine Center at Emory University for sample processing. We thank Jens Wrammert for kindly sharing the purified RBD antigen for generation of mouse anti-sera. We thank Srilatha Edupuganti for kindly providing some specimens and comments. Finally, we would like to thank all the participating patients for donating their specimens.

Appendix A. Supplementary data

Supplementary data related to this article can be found at https://doi.org/10.1016/j.virol.2021.03.009.

References

Abolghasemi, H., Eshghi, P., Cheraghali, A.M., Imani Fooladi, A.A., Bolouki Moghaddam, F., Imanizadeh, S., Moeini Maleki, M., Ranjkesh, M., Rezapour, M., Bahramifar, A., Einollahi, B., Hosseini, M.J., Jafari, N.J., Nikpouraghdam, M., Sadri, N., Tazik, M., Sali, S., Okati, S., Askari, E., Tabarsi, P., Aslani, J., Sharifipour, E., Jarahzadeh, M.H., Khodakarim, N., Salesi, M., Jafari, R., Shahverdi, S., 2020. Clinical efficacy of convalescent plasma for treatment of COVID-19 infections: results of a multicenter clinical study. Transfus. Apher. Sci. 59 https://doi.org/10.1016/j.transci.2020.102875, 102875.

Anderson, E.J., Rouphael, N.G., Widge, A.T., Jackson, L.A., Roberts, P.C., Makhene, M., Chappell, J.D., Denison, M.R., Stevens, L.J., Pruijssers, A.J., McDermott, A.B.,

Flach, B., Lin, B.C., Doria-Rose, N.A., O'Dell, S., Schmidt, S.D., Corbett, K.S., Swanson 2nd, P.A., Padilla, M., Neuzil, K.M., Bennett, H., Leav, B., Makowski, M., Albert, J., Cross, K., Edara, V.V., Floyd, K., Suthar, M.S., Martinez, D.R., Baric, R., Buchanan, W., Luke, C.J., Phadke, V.K., Rostad, C.A., Ledgerwood, J.E., Graham, B. S., Beigel, J.H., m, R.N.A.S.G., 2020. Safety and immunogenicity of SARS-CoV-2 mRNA-1273 vaccine in older adults. N. Engl. J. Med. 383, 2427–2438. https://doi.org/10.1056/NEJMoa2028436.

Asokan, M., Dias, J., Liu, C., Maximova, A., Ernste, K., Pegu, A., McKee, K., Shi, W., Chen, X., Almasri, C., Promsote, W., Ambrozak, D.R., Gama, L., Hu, J., Douek, D.C., Todd, J.P., Lifson, J.D., Fourati, S., Sekaly, R.P., Crowley, A.R., Ackerman, M.E., Ko, S.H., Kilam, D., Boritz, E.A., Liao, L.E., Best, K., Perelson, A.S., Mascola, J.R., Koup, R.A., 2020. Fc-mediated effector function contributes to the in vivo antiviral effect of an HIV neutralizing antibody. Proc. Natl. Acad. Sci. U. S. A. 117, 18754–18763.

Atyeo, C., Fischinger, S., Zohar, T., Slein, M.D., Burke, J., Loos, C., McCulloch, D.J., Newman, K.L., Wolf, C., Yu, J., Shuey, K., Feldman, J., Hauser, B.M., Caradonna, T., Schmidt, A.G., Suscovich, T.J., Linde, C., Cai, Y., Barouch, D., Ryan, E.T., Charles, R. C., Lauffenburger, D., Chu, H., Alter, G., 2020. Distinct early serological signatures track with SARS-CoV-2 survival. Immunity 53, 524–532 e524.

Barnes, C.O., West Jr., A.P., Huey-Tubman, K.E., Hoffmann, M.A.G., Sharaf, N.G., Hoffman, P.R., Koranda, N., Gristick, H.B., Gaebler, C., Muecksch, F., Lorenzi, J.C.C., Finkin, S., Hagglof, T., Hurley, A., Millard, K.G., Weisblum, Y., Schmidt, F., Hatziioannou, T., Bieniasz, P.D., Caskey, M., Robbiani, D.F., Nussenzweig, M.C., Bjorkman, P.J., 2020. Structures of human antibodies bound to SARS-CoV-2 spike reveal common epitopes and recurrent features of antibodies. Cell 182, 828–842 e816.

Bloch, E.M., 2020. Convalescent plasma to treat COVID-19. Blood 136, 654–655.

Brunner, K.T., Mauel, J., Cerottini, J.C., Chapuis, B., 1968. Quantitative assay of the lytic action of immune lymphoid cells on 51-Cr-labelled allogeneic target cells in vitro; inhibition by isoantibody and by drugs. Immunology 14, 181–196.

Chen, X.A., JL, Rostad, A.C., Ding, L., Lai, L., Mulligan, M., Rouphael, N., Natrajan, M., McCracken, C., Anderson, J.E., 2020. Development and optimization of a Zika virus antibody-dependent cell-mediated cytotoxicity (ADCC) assay. J. Immunol. Methods. https://doi.org/10.1016/j.jim.2020.112900.

de Vries, R.D., Nieuwkoop, N.J., Pronk, M., de Bruin, E., Leroux-Roels, G., Huijskens, E. G.W., van Binnendijk, R.S., Krammer, F., Koopmans, M.P.G., Rimmelzwaan, G.F., 2017. Influenza virus-specific antibody dependent cellular cytoxicity induced by vaccination or natural infection. Vaccine 35, 238–247.

Dogan, M., Kozhaya, L., Placek, L., Gunter, C., Yigit, M., Hardy, R., Plassmeyer, M., Coatney, P., Lillard, K., Bukhari, Z., Kleinberg, M., Hayes, C., Arditi, M., Klapper, E., Merin, N., Liang, B.T., Gupta, R., Alpan, O., Unutmaz, D., 2020. Novel SARS-CoV-2 specific antibody and neutralization assays reveal wide range of humoral immune response during COVID-19. medRxiv. https://doi.org/10.1101/2020.07.07.20148106.

Feeney, K.A., Putker, M., Brancaccio, M., O'Neill, J.S., 2016. In-depth characterization of firefly luciferase as a reporter of circadian gene expression in mammalian cells. J. Biol. Rhythm. 31, 540–550.

Gao, Q., Bao, L., Mao, H., Wang, L., Xu, K., Yang, M., Li, Y., Zhu, L., Wang, N., Lv, Z., Gao, H., Ge, X., Kan, B., Hu, Y., Liu, J., Cai, F., Jiang, D., Yin, Y., Qin, C., Li, J., Gong, X., Lou, X., Shi, W., Wu, D., Zhang, H., Zhu, L., Deng, W., Li, Y., Lu, J., Li, C., Wang, X., Yin, W., Zhang, Y., Qin, C., 2020a. Development of an inactivated vaccine candidate for SARS-CoV-2. Science 369, 77–81.

Gao, R., Sheng, Z., Sreenivasan, C.C., Wang, D., Li, F., 2020b. Influenza A virus antibodies with antibody-dependent cellular cytotoxicity function. Viruses 12.

Garcia, G., Arango, M., Perez, A.B., Fonte, L., Sierra, B., Rodriguez-Roche, R., Aguirre, E., Fiterre, I., Guzman, M.G., 2006. Antibodies from patients with dengue viral infection mediate cellular cytotoxicity. J. Clin. Virol. 37, 53–57.

Hassenruck, F., Knodgen, E., Gockeritz, E., Midda, S.H., Vondey, V., Neumann, L., Herter, S., Klein, C., Hallek, M., Krause, G., 2018. Sensitive detection of the natural killer cell-mediated cytotoxicity of anti-CD20 antibodies and its impairment by B-cell receptor pathway inhibitors. BioMed Res. Int. 2018, 1023490.

Haynes, B.F., Gilbert, P.B., McElrath, M.J., Zolla-Pazner, S., Tomaras, G.D., Alam, S.M., Evans, D.T., Montefiori, D.C., Karnasuta, C., Sutthent, R., Liao, H.X., DeVico, A.L., Lewis, G.K., Williams, C., Pinter, A., Fong, Y., Janes, H., DeCamp, A., Huang, Y., Rao, M., Billings, E., Karasavvas, N., Robb, M.L., Ngauy, V., de Souza, M.S., Paris, R., Ferrari, G., Bailer, R.T., Soderberg, K.A., Andrews, C., Berman, P.W., Frahm, N., De Rosa, S.C., Alpert, M.D., Yates, N.L., Shen, X., Koup, R.A., Pitisuttithum, P., Kaewkungwal, J., Nitayaphan, S., Rerks-Ngarm, S., Michael, N.L., Kim, J.H., 2012. Immune-correlates analysis of an HIV-1 vaccine efficacy trial. N. Engl. J. Med. 366, 1275–1286.

He, W., Tan, G.S., Mullarkey, C.E., Lee, A.J., Lam, M.M., Krammer, F., Henry, C., Wilson, P.C., Ashkar, A.A., Palese, P., Miller, M.S., 2016. Epitope specificity plays a critical role in regulating antibody-dependent cell-mediated cytotoxicity against influenza A virus. Proc. Natl. Acad. Sci. U. S. A. 113, 11931–11936.

Hsieh, Y.T., Aggarwal, P., Cirelli, D., Gu, L., Surowy, T., Mozier, N.M., 2017. Characterization of FcgammaRIIIA effector cells used in in vitro ADCC bioassay: comparison of primary NK cells with engineered NK-92 and Jurkat T cells. J. Immunol. Methods 441, 56–66.

Huo, J., Zhao, Y., Ren, J., Zhou, D., Duyvesteyn, H.M.E., Ginn, H.M., Carrique, L., Malinauskas, T., Ruza, R.R., Shah, P.N.M., Tan, T.K., Rijal, P., Coombes, N., Bewley, K.R., Tree, J.A., Radecke, J., Paterson, N.G., Supasa, P., Mongkolsapaya, J., Screaton, G.R., Carroll, M., Townsend, A., Fry, E.E., Owens, R.J., Stuart, D.I., 2020. Neutralization of SARS-CoV-2 by destruction of the prefusion spike. Cell Host Microbe 28. https://doi.org/10.1016/j.chom.2020.07.002.

Jackson, L.A., Anderson, E.J., Rouphael, N.G., Roberts, P.C., Makhene, M., Coler, R.N., McCullough, M.P., Chappell, J.D., Denison, M.R., Stevens, L.J., Pruijssers, A.J., McDermott, A., Flach, B., Doria-Rose, N.A., Corbett, K.S., Morabito, K.M., O'Dell, S., Schmidt, S.D., Swanson 2nd, P.A., Padilla, M., Mascola, J.R., Neuzil, K.M., Bennett, H., Sun, W., Peters, E., Makowski, M., Albert, J., Cross, K., Buchanan, W., Pikaart-Tautges, R., Ledgerwood, J.E., Graham, B.S., Beigel, J.H., m, R.N.A.S.G., 2020. An mRNA vaccine against SARS-CoV-2 - preliminary report. N. Engl. J. Med. 383, 1920–1931. https://doi.org/10.1056/NEJMoa2022483.

JKU, 2020. Maping COVID 19 Center for Systems Science and Engineering (CSSE) at. Johns Hopkins University.

Karlsson, I., Borggren, M., Jensen, S.S., Heyndrickx, L., Stewart-Jones, G., Scarlatti, G., Fomsgaard, A., 2018. Immunization with clinical HIV-1 env proteins induces broad antibody dependent cellular cytotoxicity-mediating antibodies in a rabbit vaccination model. AIDS Res. Hum. Retrovir. 34, 206–217.

Mentlik James, A., Cohen, A.D., Campbell, K.S., 2013. Combination immune therapies to enhance anti-tumor responses by NK cells. Front. Immunol. 4, 481.

Mielke, D., Bandawe, G., Pollara, J., Abrahams, M.R., Nyanhete, T., Moore, P.L., Thebus, R., Yates, N.L., Kappes, J.C., Ochsenbauer, C., Garrett, N., Abdool Karim, S., Tomaras, G.D., Montefiori, D., Morris, L., Ferrari, G., Williamson, C., 2019. Antibody-dependent cellular cytotoxicity (ADCC)-Mediating antibodies constrain neutralizing antibody escape pathway. Front. Immunol. 10, 2875.

Moeller, E., 1965. Contact-induced cytotoxicity by lymphoid cells containing foreign isoantigens. Science 147, 873–879.

Parekh, B.S., Berger, E., Sibley, S., Cahya, S., Xiao, L., LaCerte, M.A., Vaillancourt, P., Wooden, S., Gately, D., 2012. Development and validation of an antibody-dependent cell-mediated cytotoxicity-reporter gene assay. mAbs 4, 310–318.

Robbiani, D.F., Gaebler, C., Muecksch, F., Lorenzi, J.C.C., Wang, Z., Cho, A., Agudelo, M., Barnes, C.O., Gazumyan, A., Finkin, S., Hagglof, T., Oliveira, T.Y., Viant, C., Hurley, A., Hoffmann, H.H., Millard, K.G., Kost, R.G., Cipolla, M., Gordon, K., Bianchini, F., Chen, S.T., Ramos, V., Patel, R., Dizon, J., Shimeliovich, I., Mendoza, P., Hartweger, H., Nogueira, L., Pack, M., Horowitz, J., Schmidt, F., Weisblum, Y., Michailidis, E., Ashbrook, A.W., Waltari, E., Pak, J.E., Huey-Tubman, K.E., Koranda, N., Hoffman, P.R., West Jr., A.P., Rice, C.M., Hatziioannou, T., Bjorkman, P.J., Bieniasz, P.D., Caskey, M., Nussenzweig, M.C., 2020. Convergent antibody responses to SARS-CoV-2 in convalescent individuals. Nature 584, 437–442.

Shaw, A.M., Hyde, C., Merrick, B., James-Pemberton, P., Squires, B.K., Olkhov, R.V., Batra, R., Patel, A., Bisnauthsing, K., Nebbia, G., MacMahon, E., Douthwaite, S., Malim, M., Neil, S., Martinez Nunez, R., Doores, K., Mark, T.K.I., Signell, A.W., Betancor, G., Wilson, H.D., Galao, R.P., Pickering, S., Edgeworth, J.D., 2020. Real-world evaluation of a novel technology for quantitative simultaneous antibody detection against multiple SARS-CoV-2 antigens in a cohort of patients presenting with COVID-19 syndrome. Analyst 145, 5638–5646.

Singh, K., Marasini, B., Chen, X., Ding, L., Wang, J.J., Xiao, P., Villinger, F., Spearman, P., 2020. A bivalent, spherical virus-like particle vaccine enhances breadth of immune responses against pathogenic Ebola viruses in rhesus macaques. J. Virol. 94.

Singh, K., Marasini, B., Chen, X., Spearman, P., 2018. A novel Ebola virus antibody-dependent cell-mediated cytotoxicity (Ebola ADCC) assay. J. Immunol. Methods 460, 10–16.

Smalls-Mantey, A., Doria-Rose, N., Klein, R., Patamawenu, A., Migueles, S.A., Ko, S.Y., Hallahan, C.W., Wong, H., Liu, B., You, L., Scheid, J., Kappes, J.C., Ochsenbauer, C., Nabel, G.J., Mascola, J.R., Connors, M., 2012. Antibody-dependent cellular cytotoxicity against primary HIV-infected CD4+ T cells is directly associated with the magnitude of surface IgG binding. J. Virol. 86, 8672–8680.

Su, B., Dispinseri, S., Iannone, V., Zhang, T., Wu, H., Carapito, R., Bahram, S., Scarlatti, G., Moog, C., 2019. Update on fc-mediated antibody functions against HIV-1 beyond neutralization. Front. Immunol. 10, 2968.

Suthar, M.S., Zimmerman, M., Kauffman, R., Mantus, G., Linderman, S., Vanderheiden, A., Nyhoff, L., Davis, C., Adekunle, S., Affer, M., Sherman, M., Reynolds, S., Verkerke, H., Alter, D.N., Guarner, J., Bryksin, J., Horwath, M., Arthur, C., Saakadze, N., Smith, G.H., Edupuganti, S., Scherer, E.M., Hellmeister, K., Cheng, A., Morales, J.A., Neish, A.S., Stowell, S.R., Frank, F., Ortlund, E., Anderson, E., Menachery, V., Rouphael, N., Metha, A., Stephens, D.S., Ahmed, R., Roback, J., Wrammert, J., 2020. Rapid generation of neutralizing antibody responses in COVID-19 patients. Cell Rep Med 23. https://doi.org/10.1016/j.xcrm.2020.100040.

Wagstaffe, H.R., Clutterbuck, E.A., Bockstal, V., Stoop, J.N., Luhn, K., Douoguih, M., Shukarev, G., Snape, M.D., Pollard, A.J., Riley, E.M., Goodier, M.R., 2019. Antibody-dependent natural killer cell activation after Ebola vaccination. J. Infect. Dis. https://doi.org/10.1093/infdis/jiz657.

Walls, A.C., Park, Y.J., Tortorici, M.A., Wall, A., McGuire, A.T., Veesler, D., 2020. Structure, function, and antigenicity of the SARS-CoV-2 spike glycoprotein. Cell 181, 281–292 e286.

Wang, S.Y., Racila, E., Taylor, R.P., Weiner, G.J., 2008. NK-cell activation and antibody-dependent cellular cytotoxicity induced by rituximab-coated target cells is inhibited by the C3b component of complement. Blood 111, 1456–1463.

Wrapp, D., Wang, N., Corbett, K.S., Goldsmith, J.A., Hsieh, C.L., Abiona, O., Graham, B. S., McLellan, J.S., 2020. Cryo-EM structure of the 2019-nCoV spike in the prefusion conformation. Science 367, 1260–1263.

Zheng, Z., Teo, S.H.C., Arularasu, S.C., Liu, Z., Mohd-Ismail, N.K., Mok, C.K., Ong, C.B., Chu, J.J., Tan, Y.J., 2020. Contribution of Fc-dependent cell-mediated activity of a vestigial esterase-targeting antibody against H5N6 virus infection. Emerg. Microb. Infect. 9, 95–110.